JOURNAL OF MATERIALS SCIENCE 9 (1974) 383–388

Creep and stress relaxation of germanium single crystals

M. BEKIROVIC, P. FELTHAM
Department of Physics, Brunel University, Uxbridge, London, UK

Isothermal creep and stress relaxation were studied in germanium single crystals oriented for double slip at 400 to 700°C under compressive stresses of 180 to 490 kgf cm^{-2}. The curves, S-shaped in both types of experiment, were compared with corresponding-ones derived from a stochastic model involving a spectrum of energy barriers to dislocation movement. Agreement was satisfactory for stress relaxation; discrepancies in the case of creep point to the difficulty of correlating creep and stress relaxation when an equation of state is inadequate as an approximation for representing the plastic response. Differences between predicted and observed behaviour are, however, of diagnostic value concerning the extent of dislocation multiplication and other structural changes.

1. Introduction

In a recent study of the creep of germanium crystals at elevated temperatures, Chaudhri and Feltham [1] showed that a reasonable interpretation of their results was possible within the framework of a stochastic model of creep [2, 3], in which a spectrum of energy barriers, rather than a single specific barrier-type, determined the creep rate. The main object of the present work was to derive from the model more exact solutions than the "zeroth"-order ones used in [1], particularly for the representation of S-shaped creep-curves generally observed in crystals having the diamond structure, and to use it for the representation of creep as well as stress-relaxation data obtained with germanium crystals from the same stock as in [1]. By encompassing the earlier results within this program it was intended to extend the scope of the work.

2. Experimental methods and results

The germanium crystals used in all the experiments came from the same batch as those described previously [1]. They were Sb-doped with 7×10^{13} donors cm^{-3}, with an initial dislocation density of 3×10^{3} cm^{-2}, and measured $0.4 \times 0.4 \times 1.0$ cm^3. Their orientation was for multiple slip; the direction of the long, compression-axis was [1 1 0]. The rectangular sides were $(1\bar{1}1)$ and $(\bar{1}12)$. Initially the Schmid-factor for slip was 0.41 for all favoured systems. To avoid difficulties due to barrelling, plastic strains were, in all cases, limited to a few per cent.

Polishing of the crystals, the design of the vacuum furnace, and other experimental detail appertaining to the creep in compression, have been described in [1]. Stress relaxation took place in a "Nimonic 90" compression-tool encased in a cylindrical vacuum-chamber, which was seated on the guide-rails of a "Hounsfield Tensometer". Stress was automatically recorded via a sensitive inductive transducer activated by the cross-beam of the machine. The contribution of the latter to the relaxation was checked with the aid of a zirconia dummy-specimen, and was found to be negligible at all temperatures used.

Ideally, comparisons of creep and stress relaxation are best made with crystals having similar substructures, and deformation of the crystals during relaxation should be prevented altogether [4], to inhibit work-hardening effects. The first requirement was not strictly adhered to because loading a crystal for creep generally occurred within 1 to 2 sec, while periods one to two orders of magnitude longer were required to apply the same stress to a crystal in a relaxation experiment. However, earlier creep data have shown [1] that within a certain domain of stress and temperature a relatively long "incubation period" of low strain-rate preceded the onset of more rapid creep, so that the initial loading-rate

was then expected not to be of decisive significance in relation to the characteristics of the creep.

The plastic deformation sustained by specimens in the course of relaxation, following deformation to the initial compressive stress σ_0, was generally of the order of $\frac{1}{2}\%$. In view of the weak influence of the initial stress-level on the shape of relaxation curves and on the total relaxation observed within the domain of variables used, we shall not attempt to correct for any effects arising from this although, as some results, discussed below, indicate, the problem may need to be examined in detail at relatively low temperatures.

The preceding considerations led us to confine the work to temperatures and stress levels in which S-shaped creep and stress relaxation curves were observed. Combinations of the variables resulting in near-logarithmic type of curves, i.e. with high initial rates, although studied in [1], were excluded.

In a relaxation experiment the crystal, in thermal equilibrium in the compression tool, was deformed at a strain-rate of about 3×10^{-4} sec^{-1} until the desired compressive-stress level was reached. The machine was then stopped, and the relaxation was automatically recorded over periods of up to 14 h. Special attention was paid to temperature control and elimination of associated expansion-effects in the machine. Except for a special test at 450°, in which the specimen was allowed to relax at three consecutive stress levels, each crystal was allowed to relax only once. Some crystals were also pre-strained at half the above loading rate. At 470° C differences in the relaxation behaviour of crystals deformed at standard and the reduced rates, respectively, became significant only at stresses somewhat outside the range used in the runs here considered. With the lower rate the curves were slightly displaced in the positive direction of the time axis, and the extent of relaxation, as measured after 3×10^4 sec, was about 10% lower than in the corresponding case for the more rapidly pre-strained crystal.

In comparing creep and stress-relaxation data, results from first runs, in which the initial structures can be regarded as reasonably similar in creep and corresponding stress-relaxation specimens, are most directly relevant for purposes of comparison. The effect of structural changes is apparent from Fig. 1, in which all three curves were obtained with the same

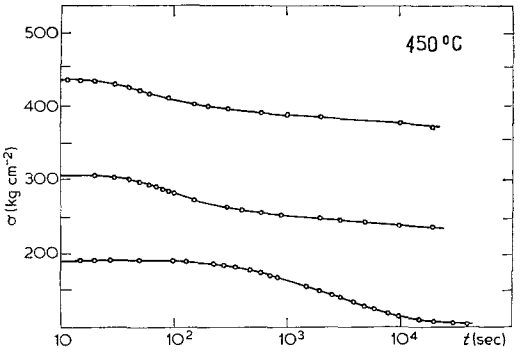

Figure 1 A sequence of stress-relaxation curves obtained with a single specimen, showing the progressive reduction in total relaxation, and a "shift" of the curves to the left on repeated relaxation.

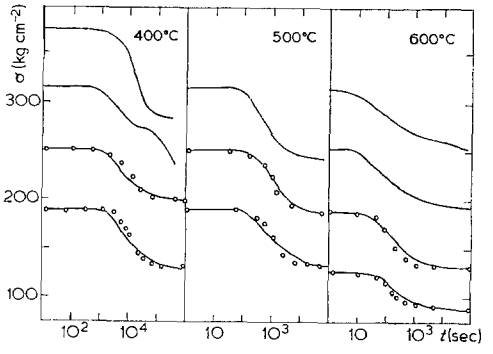

Figure 2 Stress relaxation curves in compression at three temperatures. A new crystal was used for each curve. The lines represent measurements; the points are "theoretical".

crystal. Successive curves are seen to be progressively displaced towards the left as the initial stress-level is raised. At the same time the total extent of relaxation decreases, suggesting a more flow-resistant, work-hardened structure at the higher stress-levels. This feature is much less pronounced in the sets where each run was carried out with a new crystal (Fig. 2). The continuous curves, just like the corresponding ones for creep in Fig. 3, represent measurements; the points shown associated with them in both figures were obtained by means of the theoretical model, as will be shown below.

An uninterrupted stress/deformation curve, in which the crystal deformed at the standard strain-rate, transcribed from the drum-chart of the Hounsfield Tensometer (Fig. 4) shows the relation between the cross-head traverse and the stress acting on the crystal to be approximately

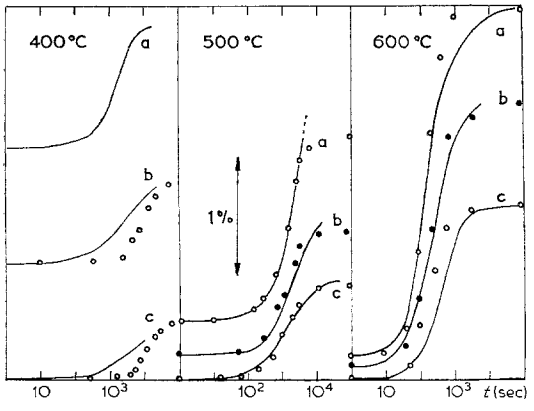

Figure 3 Compressive creep at three temperatures. A new crystal was used for each experiment. The origins of the strain axis have been displaced arbitrarily for convenience of representation. Full lines represent measurements; the points are "theoretical". Compressive stresses were (a) 313, (b) 250 and (c) 188 kgf cm^{-2}.

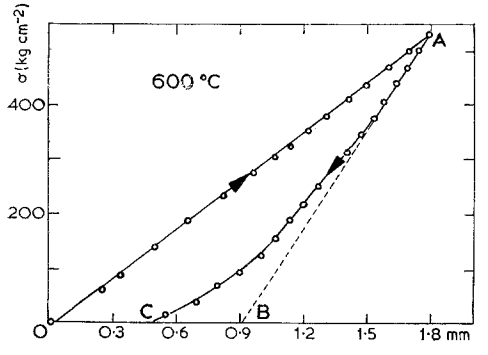

Figure 4 A loading-unloading record for a crystal compressed in the "Hounsfield Tensometer", indicating the anelastic (BC) and plastic (CO) parts of the deformation.

linear on loading to a stress level including and exceeding those used in any relaxation run. The cross-head traverse here includes a significant elastic contribution from the machine which, together with the elastic part of the deformation of the crystal, defines the slope of the tangent at the point A, i.e. that of the line AB in the figure. The time-dependent, anelastic part of the deformation of the specimen, following unloading at about the same absolute rate as used in loading along OA, is represented by BC. The irreversible, plastic strain, equal to about 3% in this case, is indicated by OC. Thus extensive relaxation can be seen to have taken place in the course of unloading, i.e. during about $2\frac{1}{2}$ min. This is qualitatively in agreement with the substantial drop in the stress during relaxation at 600°C, apparent from Fig. 2.

Some observations of the dislocation substructure developing in the crystals during creep were reported in [1]; no further TEM studies were made.

3. Theory

Interpretation of creep data in [1] was based on a stochastic model of dislocation kinetics [2], which has since been developed further [3]. The choice of this model for the interpretation of creep and, by implication, stress-relaxation, particularly its suitability for crystals with the diamond structure, has been discussed before [1]; we therefore outline only its basic features as a preliminary to the derivation of a new solution representing S-shaped creep and stress-relaxation curves, which is not restricted in its scope by the rather severe approximations previously made.

In the model referred to [2, 3], an activated jump of a slip unit, for example of a dislocation segment pinned at a localized obstacle as indicated in Fig. 5, is assumed to take it from a barrier of height u, lying within a spectrum $u_{\min} \leqslant u \leqslant u_{\max}$, to a new one. The latter may be either higher or lower than u by a "small" fixed amount δu, which is taken to be constant in any given creep experiment.

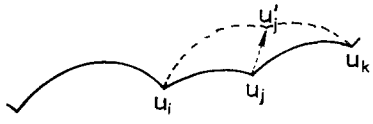

Figure 5 Transition of a dislocation segment between localized barriers.

In view of the assumed randomness of the internal stress-field, the chance of a jump to a higher barrier is taken equal to the probability of a transition to a lower one. By considering three consecutive energy-intervals, as shown in Fig. 6, a differential equation is obtained for the number $n(u, t).\delta u$ of such states per unit volume

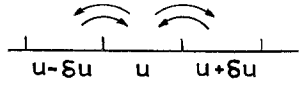

Figure 6 Possible transitions from and to a given energy level in the barrier-height distribution.

of the crystal at time t after the onset of creep. The equation is then transformed by using the transition-probability density defined by $N(u, t) = n(u, t) \cdot \exp(-u/kT)$, leading to the relation

$$\frac{\partial N}{\partial t} = e^{-u/kT} D \frac{\partial^2 N}{\partial u^2}, \qquad D = \tfrac{1}{2} \nu (\delta u)^2 = \text{constant} \quad (1)$$

where ν is a vibrational frequency of the order of 10^{10} sec^{-1} [5]. Equation 1 can be regarded as the Fokker-Planck equation of an Ornstein-Uhlenbeck process in the stochastic variable N [6].

A solution of Equation 1 suitable for the present purpose is obtained by the following successive steps. First Equation 1 is rewritten in terms of s, where $s = \exp(u/kT)$. Then variables are separated by writing $N(s, t) = N_1(s) \cdot N_2(t)$. Finally, on expressing N_1 in terms of the new variable r, where $r = s^{\frac{1}{2}}$, one obtains N_1 as a Bessel equation of order zero in r, and N_2 as an exponential term in t.

We shall first consider a solution which leads to a constantly diminishing creep rate, and then generalize it to include curves of the required S-shape. It will be convenient, for purposes of discussion, to work with the variables r and t.

The first solution referred to is given by the Fourier-Bessel series

$$N(r, t) = \sum_{i=1}^{\infty} A_i e^{-t/t_i} J_0(\alpha_i r), \quad (2)$$

where

$$t_i = D^{-1} (2kT/\alpha_i)^2, \quad (3)$$

$$A_i \propto 1/[\alpha_i J_1(\alpha_i r_{\max})], \quad (4)$$

and the α_i's are the positive roots of $J_0(\alpha r_{\max})$; $r_{\max}$ corresponds to the largest u-value in the operative spectrum, i.e. the transition probability for jumps over barriers higher than $u = u_{\max}$ is negligible within the period of the creep test: such states remain "frozen-in". The minimum u-value is taken to be zero. This assumption is made for convenience, but is not essential. It may not be suitable in the case of heavily pre-strained crystals. J_0 and J_1 denote Bessel functions of the zeroth and first order, respectively.

Equation 2 is the complete analogue of that representing the temperature $N(r, t)$ in an infinite cylinder of radius $r_{\max}$, initially at a constant temperature throughout, the surface of which is cooled to zero at $t = 0$, and then held invariant at this, new, level [7]. A graphical representation of the function is given by Carslaw and Jaeger [7]. For any given value of r, N decreases with time; the curve is S-shaped. The creep resulting from such a distribution is readily shown to be of the continuously-decelerating type, but we do not propose to examine it here further. However, we shall use Equation 2 in the representation of S-shaped creep curves.

We note, first, that Equation 1 is invariant with respect to a displacement of the origin along the time axis, i.e. with t_0 constant,

$$\frac{\partial N}{\partial (t + t_0)} = \frac{\partial N}{\partial t}, \quad (5)$$

It follows that $N(r, t + t_0)$, expressed in the same form as Equation 2, but with t replaced everywhere by $t + t_0$, is also a solution of Equation 1. As Bessel's equation is linear, N_s, given by

$$N_s = N(r, t) - N(r, t + t_0) \quad (6)$$

also satisfies Equation 1. For any given r-value the form of N_s is bell-shaped. This is readily seen by considering "small" values of t_0, when, as is apparent from Equation 6 (remembering that N, for fixed r, is S-shaped),

$$N_s \approx t_0 \frac{\partial N}{\partial t}. \quad (7)$$

Now if, in accord with [2], each activated jump, e.g. of a dislocation segment, is assumed to make the same "average" contribution to the overall shear-strain, then the strain-rate is proportional to the integral of the transition probabilities either over the u-spectrum or over the corresponding range of r-values, depending upon the representation used. With the form of N given by Equation 2, integration of N_s with respect to r leads to a series of exponential terms in the time variable, of positive and negative signs, the pre-exponential coefficients in which depend on i, $r_{\max}$ and t_0. The plastic shear-strain is then obtained, from the strain-rate evaluated in this manner, by integration with respect to time. Clearly, the resulting equation again consists of a series of exponential terms, i.e. we may write formally

$$\gamma = \gamma_0 \sum_{i=1}^{\infty} C_i (1 - e^{-t/t_i}) \quad (8)$$

with

$$\gamma_0 = \gamma(\infty) / \sum_{i=1}^{\infty} C_i, \quad (9)$$

the C_i co-efficients depending on r_{max} and t_0; $\gamma(\infty)$ represents the strain attained asymptotically as $t \to \infty$. Its dependence on stress and temperature is not pronounced, as may be inferred from Fig. 3; this has been discussed briefly in [1], and will not be analysed further.

The form of the C_i-terms is readily established on the basis of the steps taken in deriving Equation 8 from Equation 6, but as the terms depend on the boundary conditions, i.e. on t_0 and on the extrema of the u-spectrum, as seems to be confirmed by Fig. 1, generalizations about these coefficients, useful at the present stage of development of the theory, cannot be readily made. We shall revert to the use of Equation 8 for the analysis of creep data below, after considering its relevance to stress relaxation.

Now, in the ideal case, when stress relaxation in shear occurs at constant strain, the sum of the "elastic" and "plastic" shear rates is zero, i.e.

$$\dot{\gamma}_{el} + \dot{\gamma} = 0\,, \qquad (10)$$

where the elastic strain-rate is equal to $\dot{\tau}/G$, τ being the shear stress and G the shear modulus. It follows that in the equation representing the plastic shear-rate, the latter may be replaced by $-\dot{\tau}/G$ at the time when the total strain-rate is reduced to zero. Then, proceeding as in the case of creep discussed above, one obtains instead of Equation 8

$$\frac{\tau(0) - \tau(t)}{\tau(0) - \tau(\infty)} = \frac{\sum_{i=1}^{\infty} C_i(1 - e^{-t/ti})}{\sum_{i=1}^{\infty} C_i}\,, \qquad (11)$$

showing the identity of the functional forms of the creep and stress relaxation Equations 8 and 11.

Writing $\Delta\tau(t)$ for the numerator of the left-hand side of Equation 11, one obtains, on using Equations 8 and 9:

$$\Delta\tau = K\gamma(t)\;;\; K = \Delta\tau(\infty)/\gamma(\infty)\,. \qquad (12)$$

The shear stresses and strains appearing in Equations 8 to 11, including $\tau(\infty)$ and $\gamma(\infty)$, can be replaced in both equations by corresponding compressive stresses and strains respectively.

We note that the derivation of Equation 11, and equally of Equation 8, by integration of rate equations with respect to time, implies that structural changes, other than those encompassed by the postulates of the model, do not occur in the course of creep and stress relaxation. This may be a reasonable assumption at relatively low temperatures, when recovery processes are essentially of the "dynamic" type. At elevated temperatures diffusion-induced structural changes may however occur. These may be more pronounced in a creep test at a certain constant stress compared with those in a relaxation test in which the stress is only initially at the same constant level. Dislocation multiplication and other stress-sensitive effects contributing to the plastic response of the crystal may, in that case, be rather less intense. K, in Equation 12 would then be expected to decrease with increasing temperature. The evidence in Figs. 2 and 3, appertaining to the total extent of relaxation, and to the final strains attained in creep, provide some support for this view. Consequently, correlations between creep and stress-relaxation, as represented by Equations 8 and 11 for example, may prove of diagnostic value of the stress sensitivity and other features of the micro-mechanics of plasticity at elevated temperatures.

4. Experimental results in the light of the model

In order to investigate the extent of the applicability of the model, particularly Equations 8 and 11, to the creep and stress-relaxation data obtained in [1] and in the present work, the following procedure was adopted. Firstly, curves of S-shaped form, complying with Equation 8, were fitted empirically to experimental creep data obtained in [1] at a constant stress over a relatively wide temperature range. A reasonable fit was obtained by using only two terms of the

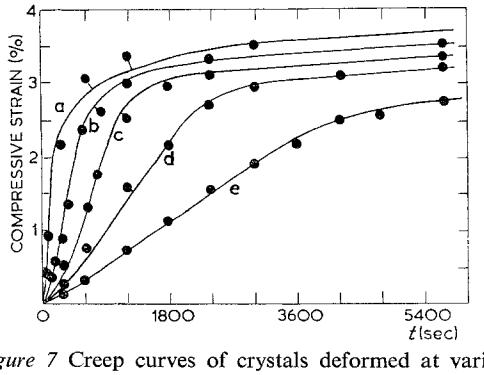

Figure 7 Creep curves of crystals deformed at various temperatures at a compressive stress of 485 kgf cm^{-2}. Measurements, taken from [1], are indicated by full lines; the points were obtained by means of Equation 8, using two terms only. Values of C_2/C_1 were, on going from (a) to (e), -0.20, -0.20, -0.30, -0.38 and -0.30, respectively. The times t_1 and t_2 are given in Fig. 8.

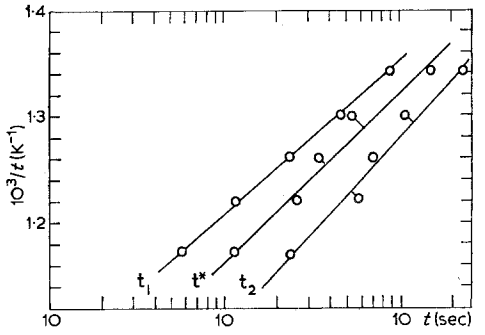

Figure 8 The times t_1 and t_2 used in the evaluation of the data shown by points in Fig. 7. The times t^* appertain to the calculated inflexion points of the curves.

series, as is apparent from Fig. 7 in which the full lines represent measurements, while the points were obtained with the aid of Equation 8.

Values of t_1 and t_2 which were substituted into Equation 8 are indicated in Fig. 8, together with t^*, which corresponds to the calculated inflexion-points of the curves. The slopes of the lines in Fig. 8 yield, with the usual Arrhenius analysis, "activation energies" of 1.1 to 1.4 eV, agreeing reasonably well with the value of about 25 kT suggested by the model [1] for the most probable barrier height in the spectrum; at 500°C 25 kT $\approx$ 1.6 eV.

Secondly, by interpolation and extrapolation, values of t_1 and t_2 were derived from the lines in Fig. 8 for the temperatures at which the experimental results represented in Figs. 2 and 3 were obtained. They are shown in Table I together with the approximate C_2/C_1 values. The latter corresponded to the C_2/C_1-ratios used, at nearly the same temperatures, for the evaluation of the "theoretical" points in Fig. 7. The value of C_2/C_1 for 400°C was obtained by extrapolation of the, apparently near-linear, curve representing the temperature dependence of this ratio, based on the few values used in Fig. 7.

TABLE I Parameters used in Equations 8 and 11 to obtain the calculated values shown by points in Figs. 2 and 3. The times are given in seconds.

°C	t_1	t_2	t^*	C_2/C_1
400	12000	7800	9800	−0.54
500	1080	480	565	−0.38
600	27	168	72	−0.20

The "theoretical" results, denoted by points in Figs. 2 and 3, show rather good agreement with the experimental curves in the case of stress relaxation at the lower stress-levels. At higher stresses, probably as a result of severe structural changes induced during loading, the agreement on using the same parameters as for the low-stress curves was less satisfactory, and the points have not been drawn in. An anomalously "wavy" curve was found in the relaxation from the 313 kgf cm^{-2} level at 400°C; the same instability occurred on repeating the run with a new crystal.

5. Conclusions

Solutions representing S-shaped creep and stress relaxation curves, derived from a stochastic model of crystal plasticity [2, 3], were found to provide a foundation for the representation and study of creep and stress relaxation in germanium crystals at elevated temperatures. Some weaknesses of the analysis reside in the simplifications which were necessary originally to make the theory tractable, as well as in the present application of the theory to experiment. In particular some lack of rigour was unavoidable in the transition from the "full" equation deduced from the model, i.e. Equation 6, to the two-term approximation used in the analysis of the data. While these, and other, points need further attention, the present approach nevertheless seems potentially rewarding from the point of view of the interpretation of creep and stress relaxation in solids as evolutionary stochastic processes.

References

1. G. CHAUDHRI and P. FELTHAM, *J. Mater. Sci.* **7** (1972) 1161.
2. P. FELTHAM, *Phys. Stat. Sol.* **30** (1968) 135.
3. *Idem, J. Phys. (London) D* **6** (1973) 2048.
4. R. W. ROHDE and T. V. NORDSTROM, *Scripta Met.* **7** (1973) 317.
5. H. KRONMÜLLER, *Phys. Stat. Sol. B*, **52** (1972) 231.
6. J. K. E. TUNALEY, *J. Appl. Phys.* **43** (1972) 4777.
7. H. S. CARSLAW and J. C. JAEGER, "Conduction of Heat in Solids" (Oxford University Press, Oxford, 1948) p. 171.

Received 21 August and accepted 10 October 1973.